Supporting Information

Hayashi et al. 10.1073/pnas.1419767112

SI Materials and Methods

Antibodies. Antibodies were purchased as follows: Cox4 (Abcam; ab14744), Cox5a (Abcam; ab110262), Cox5b (Abcam; ab110263), Cor1 (Abcam; ab110252), actin (Santa Cruz; sc-1615), HIGD1A (Proteintech; 21749-1-AP), Flag (Sigma; F1804), Vdac (Abcam; ab14734), and Alexa 488- and Alexa 568-labeled secondary antibodies (Invitrogen; A-11001, A-11034, and A-11004). Polyclonal antibodies against Higd1a were generated by immunization with a peptide corresponding to rat Higd1a amino acid sequence (amino acids 2–18, STNTDLSLSSYDEGQGSC) in rabbit.

Cell Culture. Cardiomyocytes obtained from 1-or 2-d-old Wister rats were prepared and cultured in DMEM (Invitrogen) containing 10% (vol/vol) FBS and 100 units/mL penicillin-streptomycin-glutamine. Cells were cultured under 5% CO_2 at 37 °C. For hypoxic exposure, cells were placed in a MCO-5M multigas incubator (Sanyo).

Microarray Data Analysis. Data analysis and normalization were previously mentioned (1). In brief, data analysis was performed using the GeneSpring GX 12.5 bioinformatics software (Agilent Technologies), using the latest gene annotations available. One-way ANOVA test was applied to the filtered gene list, resulting in a group of genes with significant differences. A hierarchical clustering method (heat map constructions) was used to group genes on the basis of similar expression patterns over all samples. Comparisons of the lists of up-regulated genes among them were performed by Venn diagrams.

Constructs. The coding sequence of rat *Higd1a* (NM_080902.3) was amplified by PCR from neonatal rat heart cDNA and cloned into pENTR/D-TOPO (Invitrogen). Next, carboxyl terminus Flag tag was fused by PCR. For adenoviral construction, we used the ViraPower Adenoviral Expression system (Invitrogen) and the BLOCK-iT Adenoviral RNAi Expression system for shRNA (Invitrogen). For shRNA construction, shRNA oligonucleotides were designed as synthetic duplexes with overhanging ends identical to those created by restriction enzyme digestion site. Each oligonucleotide containing a target sequence was subcloned into pENTR-U6 and recombined into pAd/BLOCK-iT-DEST. The target of shRNA for *Higd1a* is the 5′-UTR. The sequences used are as follows: shRNA for *Higd1a*, ccgaagactcttcaagaaa and shRNA for *LacZ*, ctacacaaatcagcgattt. The adenoviral particles were produced by transfection in 293A cells.

Immunoprecipitation. Cardiomyocytes were collected in isotonic buffer (pH 7.4, 25 mM Hepes, 250 mM sucrose, 1 mM EDTA) and mitochondrial pellets were isolated from cell cultures as described (2) with slight modification. Mitochondrial pellets were lysed with lysis buffer (pH 7.4, 30 mM Mops, 150 mM NaCl, 1 mM EDTA, 5% (vol/vol) glycerol containing 1% *n*-dodecyl-β-D-maltoside (DDM)) for 30 min at 4 °C. After a clarifying spin, samples were incubated with individual antibodies for 2 h at 4 °C followed by addition of protein G Sepharose (GE Healthcare) for 30 min at 4 °C. After washing, the bound proteins were eluted with SDS/PAGE sample buffer.

Immunoblotting. The 200×10^4 cardiomyocytes treated under 1% oxygen were lysed in pH 7.4, 30 mM Mops, 150 mM NaCl, 1 mM EDTA, 5% (vol/vol) glycerol, 1% DDM, protease inhibitor mixtures (Amresco). After centrifugation for 5 min at 21,900 × *g* to remove insoluble material, lysates were assessed for protein levels using the BCA method (Pierce) and 4 μg of soluble protein from each was resolved on 12% Bis-Tris gels 160 V for 45 min. Gels were transferred to PVDF and Western blotted.

Immunofluorescence Assay. Cardiomyocytes were seeded on collagen-coated 35-mm glass dishes (Asahi Techno Glass). After 24 h from seeding, the cells were washed once with PBS and fixed with 4% paraformaldehyde for 10 min. The cells were permeabilized with 100% methanol for 10 min and then immunostained with anti-Higd1a polyclonal antibody and anti-Cox4 monoclonal antibody. For secondary reactions, Alexa 488- or 568-labeled secondary antibodies (Invitrogen) were used.

The cells infected with adenovirus encoding carboxyl terminus Flag-tagged Higd1a (adHig), were treated with 50 nM of Mito-Tracker Red for 30 min, washed once with prewarmed PBS, and fixed using the same method described as above. For lebeling, anti-Flag M2 monoclonal antibody (Sigma-Aldrich) was used. Fluorescence images were recorded with an Olympus FV1000D confocal microscope using a PL APO 60×, 1.35 N.A. oil immersion objective lens (Olympus).

Pull-Down Assay. Cytochrome *c* oxidase from bovine heart was purified by the method reported previously (3–5). Recombinant MBP-Higd1a (5 μg) and highly purified cytochrome *c* oxidase (hpCcO) (20 μg) were incubated at 25 °C for 30 min in the presence of 0.2% *n*-decyl-β-D-maltoside (DM), and amylose resin was added at 4 °C for 1 h. After washing, bound proteins were eluted by SDS/PAGE sample buffer.

Blue Native PAGE. A total of 10 μg of mitochondrial pellets, as measured by using the Bradford method, from cardiomyocytes was solubilized, containing 2% (wt/vol) digitonin. Solubilized samples were incubated on ice for 10 min and centrifuged for 30 min at 100,000 × *g* at 4 °C. Supernatants were added to Coomassie G-250 and resolved on a 4–16% Native PAGE Bis-Tris gel (Invitrogen). Initially run for 30 min with a constant voltage of 150 V using a cathode buffer (pH 7.0, 50 mM tricine, 7.5 mM imidazole, and 0.02% Coomassie G-250) and anode buffer (pH 7.0, 7.5 mM imidazole). Next, the cathode buffer was exchanged into the light cathode buffer (pH 7.0, 50 mM tricine, 7.5 mM imidazole, 0.002% Coomassie G-250) and run for another 75 min with a constant voltage of 150 V. After electrophoresis, proteins were transferred to PVDF membrane (0.45 μm, Millipore) using Mini Trans-Blot Cell Assembly (BIO-RAD, pH 8.3, 25 mM tricine, 192 mM glycine) with a constant voltage of 30 V.

Recombinant MBP-Higd1a and hpCcO were incubated at 25 °C for 30 min in the presence of 0.2% DM. The mixed solution was resolved by the same electrophoresis method and transferred to PVDF membrane by semidry method (pH 8.3, 25 mM tricine, 192 mM glycine, 20% (vol/vol) methanol, 0.04% SDS) for 60 min with a constant voltage of 15 V. Then, membranes were washed with 8% (vol/vol) acetic acid followed by deionized-distilled water. Each antibody was conjugated and detected with a CCD camera-based detection system (ImageQuant LAS-4000, GE Healthcare).

Measurement of Intact Cellular Respiration. Oxygen consumption rates were measured by XF96 Extracellular Flux Analyzer (Seahorse Bioscience) in unbuffered DMEM containing 25 mM glucose, 2 mM-L-glutamine, and 1 mM sodium pyruvate under basal conditions and in response to 1 μM oligomycin A, 0.5 μM fluorocarbonyl cyanide phenylhydrazone (FCCP) and 100 nM rotenone + 100 nM antimycin A (Sigma). For measurement, 6×10^4 cardiomyocytes were treated with each adenovirus (adLacZ or adHigd1a or shLacZ or shHigd1a).

Measurement of ATP Synthesis in Permeabilized Cardiomyocytes. Speed of ATP synthesis in cardiomyocytes (1.2×10^4 cells per well for shRNA-treated groups and 7.5×10^3 cells per well for adLacZ or adHigd1a-treated groups) permeabilized with 2% (wt/vol) digitonin was measured as described previously (6). In brief, after addition of assay buffer, the luminescence (produced ATP) was measured every minute for 15 min using ATP bioluminescence assay kit CLS II (Roche). Every time point of data was divided by a value of ATP production at 10 min in shLacZ or adLacZ groups. ATP production at 10 min in shLZ or adLZ was regarded as 1.0.

Cell Viability. A total of 5×10^5 cells of cardiomyocytes were transfected with either shHigd1a (shHig) or shLacZ (shLZ), cultured for 60 h, and then subjected to hypoxic conditions (1% oxygen) for another 24 h. After hypoxia, the cells were stained with 2 μg/mL propidium iodide (Sigma) and 2 μg/mL Hoechst 33342 (Dojin Chemical) at 37 °C for 30 min. The cells were analyzed using IN Cell Analyzer 6000 (GE Healthcare).

Structure Modeling. A docking model of the CcO and Higd1a was constructed as follows: The initial docking model was created in COOT (7) using the coordinates for the COX (Protein Data Bank, PDB: 3ABM, removal of TG1 and TG3) and the HIGD1A (PDB: 2LOM, model 6 of 20 structures) and then refined by energy minimization without any structure factor terms by the Crystallography and NMR system (8, 9).

Statistical Analyses. The comparison between two groups was made by *t* test (two tailed). For MASC assay, comparison was made by repeated two-way ANOVA. A value of $P < 0.05$ was considered statistically signifcant. Data represent mean ± SEM.

1. Kioka H, et al. (2014) Evaluation of intramitochondrial ATP levels identifies G0/G1 switch gene 2 as a positive regulator of oxidative phosphorylation. *Proc Natl Acad Sci USA* 111(1):273–278.
2. Klement P, Nijtmans LG, Van den Bogert C, Houstěk J (1995) Analysis of oxidative phosphorylation complexes in cultured human fibroblasts and amniocytes by blue-native-electrophoresis using mitoplasts isolated with the help of digitonin. *Anal Biochem* 231(1):218–224.
3. Tsukihara T, et al. (1995) Structures of metal sites of oxidized bovine heart cytochrome c oxidase at 2.8 A. *Science* 269(5227):1069–1074.
4. Shinzawa-Itoh K, et al. (1995) Effects of ethyleneglycol chain length of dodecyl polyethyleneglycol monoether on the crystallization of bovine heart cytochrome c oxidase. *J Mol Biol* 246(5):572–575.
5. Yoshikawa S, Choc MG, O'Toole MC, Caughey WS (1977) An infrared study of CO binding to heart cytochrome c oxidase and hemoglobin A. Implications re O2 reactions. *J Biol Chem* 252(15):5498–5508.
6. Fujikawa M, Yoshida M (2010) A sensitive, simple assay of mitochondrial ATP synthesis of cultured mammalian cells suitable for high-throughput analysis. *Biochem Biophys Res Commun* 401(4):538–543.
7. Emsley P, Lohkamp B, Scott WG, Cowtan K (2010) Features and development of Coot. *Acta Crystallogr D Biol Crystallogr* 66(Pt 4):486–501.
8. Brunger AT (2007) Version 1.2 of the Crystallography and NMR system. *Nat Protoc* 2(11):2728–2733.
9. Brünger AT, et al. (1998) Crystallography & NMR system: A new software suite for macromolecular structure determination. *Acta Crystallogr D Biol Crystallogr* 54(Pt 5): 905–921.
10. Acín-Pérez R, Fernández-Silva P, Peleato ML, Pérez-Martos A, Enriquez JA (2008) Respiratory active mitochondrial supercomplexes. *Mol Cell* 32(4):529–539.

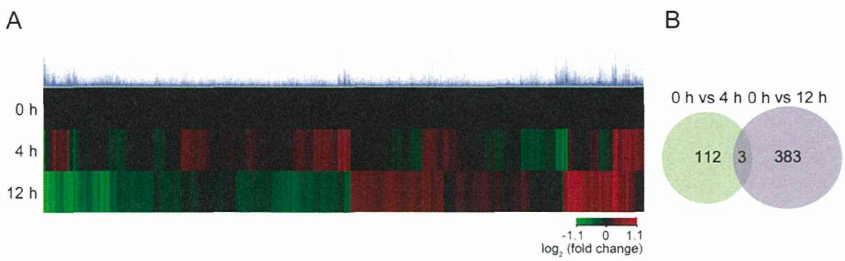

Fig. S1. Three genes were identified by microarray analysis using hypoxia-treated cardiomyocytes. (*A*) Hierarchical clustering image representing 2,598 genes exhibited significantly ($P < 0.05$; ANOVA) different expression levels at each of three time points (0, 4, and 12 h). (*B*) The Venn diagrams represented the overlap of genes that were up-regulated (>2.0-fold change up-regulated) at 4 h and genes that down-regulated (<1.2-fold change) by 12 h compared with 0 h, respectively.

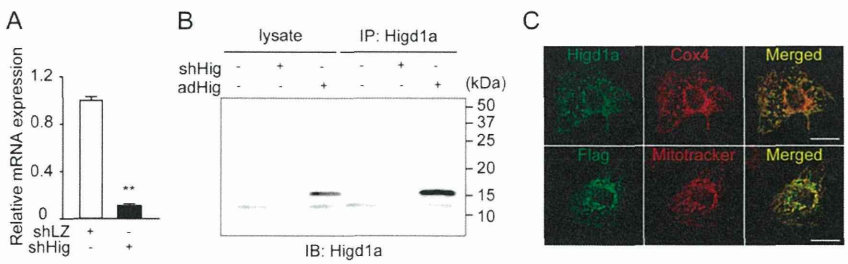

Fig. S2. Validation of our raised antibody against Higd1a. (*A*) Rat cardiomyocytes transfected with either shLacZ (shLZ) or shHigd1a (shHig) were analyzed by quantitative RT-PCR. *Higd1a* mRNA level was normalized by *Actb*. Data represent means ± SEMs ($n = 8$); $^{**}P < 0.01$, compared with control shLZ. (*B*) Validation of our established antibody for rat Higd1a. Immunoprecipitation was followed by immunoblot analysis of cardiomyocytes treated with shHig or adenovirus encoding carboxyl terminus Flag-tagged Higd1a (adHig). (*C, Upper*) Endogenous Higd1a was stained in cardiomyocytes with anti-Higd1a (green) and anti-Cox4 (red). (*Lower*) Cardiomyocytes transfected with adHig were stained with anti-Flag (green) and MitoTracker (red). The established antibody specifically recognizes neonatal rat Higd1a, which cannot be detected by commercially available Higd1a antibody (Scale bars, 20 μm.)

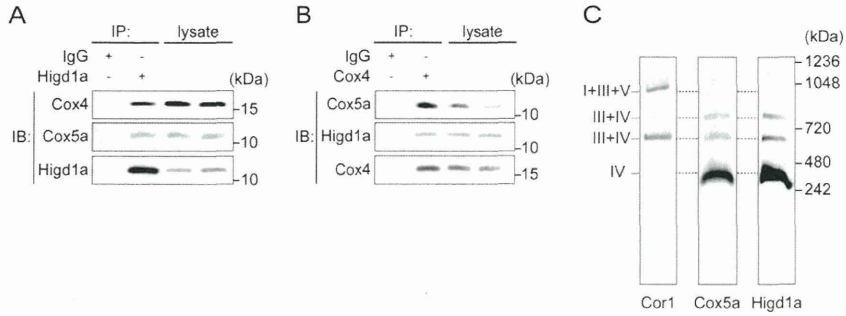

Fig. S3. Higd1a associated with CcO in rat cardiomyocytes. (*A*) Mitochondrial fractions isolated from rat cardiomyocytes were lysed and immunocaptured using an anti-Higd1a antibody and then immunoblotted with anti-Cox4 or anti-Cox5a antibodies to detect CcO subunits. (*B*) Reciprocal coimmunoprecipitation with an anti-Cox4, one of the subunits of CcO. (*C*) Mitochondrial fraction from rat cardiomyocytes was solubilized in 2% (wt/vol) digitonin and resolved by BN-PAGE, followed by immunoblotting with anti-Cox5a to detect complex IV or anti-Cor1 to detect complex III or anti-Higd1a. Higd1a integrated into the CcO, as it behaved similar to Cox5a, not to Cor1.

Fig. S4. Alignment of human Higd1a and bovine Higd1a with ClustalW (v 2.1). Black boxes, identical residues in both species; gray boxes, similar amino acids. Sequences of Higd1a are almost matched between human and bovine.

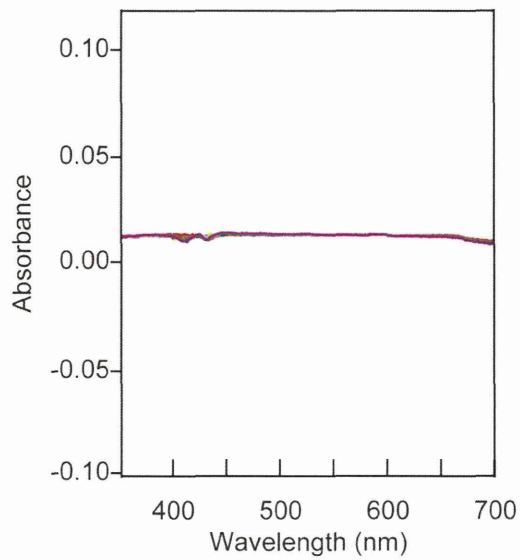

Fig. S5. Supporting data for Fig. 2. Optical absorption intensity changes of oxidized hpCcO spectra are plotted at 1 min (red), 5 min (brown), 10 min (dark yellow), 15 min (green), 20 min (light blue), 25 min (blue), and 30 min (purple) after adding MBP.

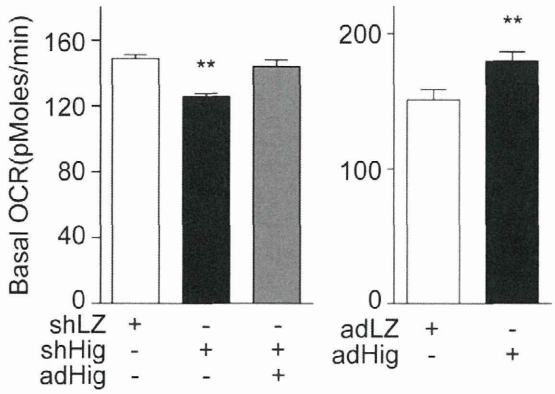

Fig. S6. Supporting data for Fig. 3. Basal oxygen consumption of rat cardiomyocytes transfected with either shLZ for control, shHig, or both shHig and adHig (n = 20 for each group).

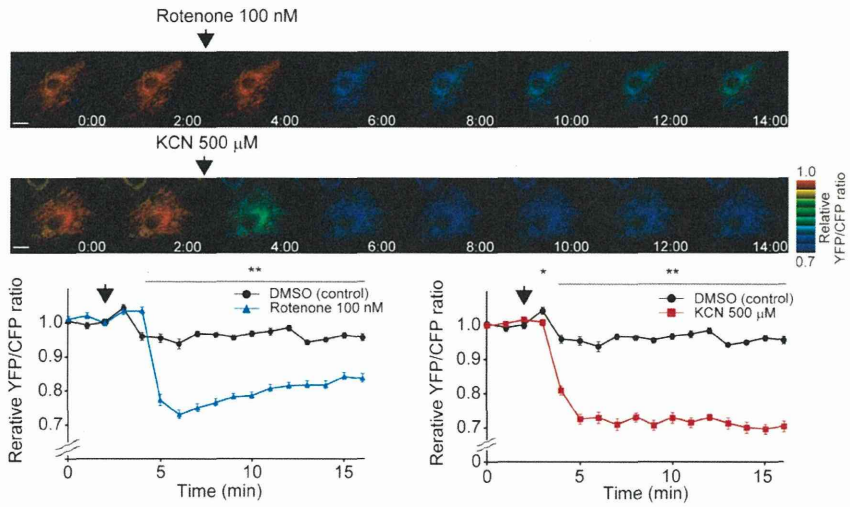

Fig. S7. Mit-ATeam assay reflects the function of complex I or IV. Mit-ATeam assay in rat cardiomyocytes is highly sensitive to assess the effect of inhibitors of rotenone (inhibitor of complex I) or KCN (inhibitor of complex IV) on mitochondrial oxidative phosphorylation. *Lower* line graphs represent YFP/CFP emission ratio plots of Mit-ATeam in rat cardiomyocytes. Rotenone (100 nM) or KCN (500 μM) was added at 2 min (arrowhead; n = 8), respectively. All measurements were normalized to the YFP/CFP emission ratio at 0 min. Data represent means ± SEMs. (Scale bars, 20 μm.)

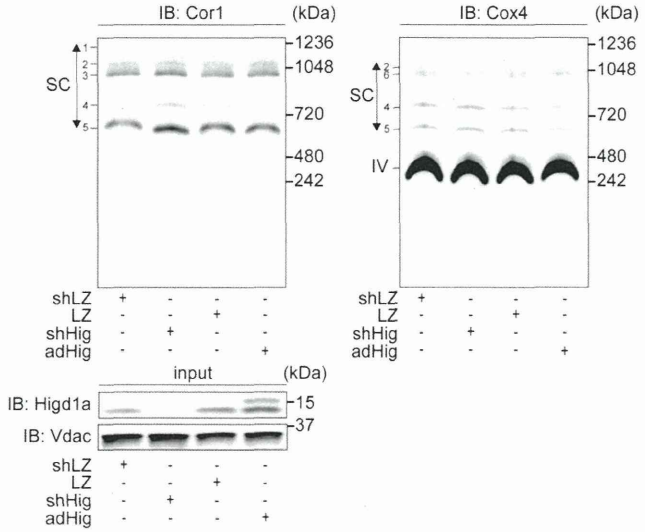

Fig. S8. Higd1a does not affect respiratory supercomplex formation. Mitochondrial fraction from rat cardiomyocytes transfected with corresponding viruses was solubilized in 2% (wt/vol) digitonin and 8 μg of each fraction was subjected to BN-PAGE, followed by immunoblotting with anti-Cox4 to detect complex IV or anti-Cor1 to detect complex III. The numbers, which are located on the *Left* side of the two *Upper* Western blots, represent respiratory supercomplex, specifically: 1 (I + III + V); 2 (I + II + III + IV); 3 (I + III + V); 4 (III + IV); 5 (III + IV); and 6 (I + III + IV) (10). *Lower* blot represents SDS/PAGE of inputs. Loading control, blotted with anti-VDAC antibody.

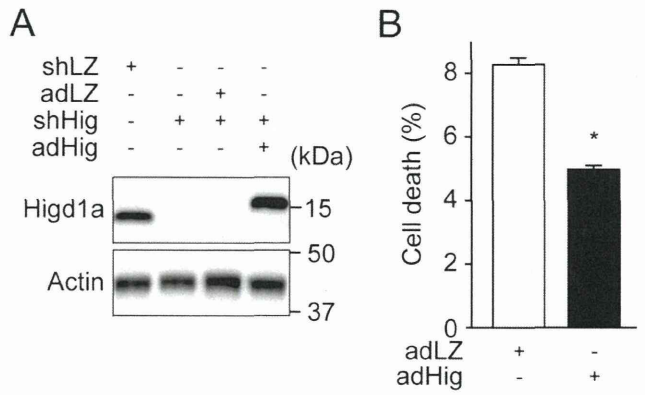

Fig. S9. Supporting data for Fig. 4*B*. (*A*) Immunoblotting of Higd1a treated with corresponding adenoviruses. (*B*) The cell viability was increased by exogenous adHig compared with adLZ under hypoxia for 14 h. Data represent means ± SEMs. $*P < 0.05$, $**P < 0.01$, compared with control (adLZ or shLZ).

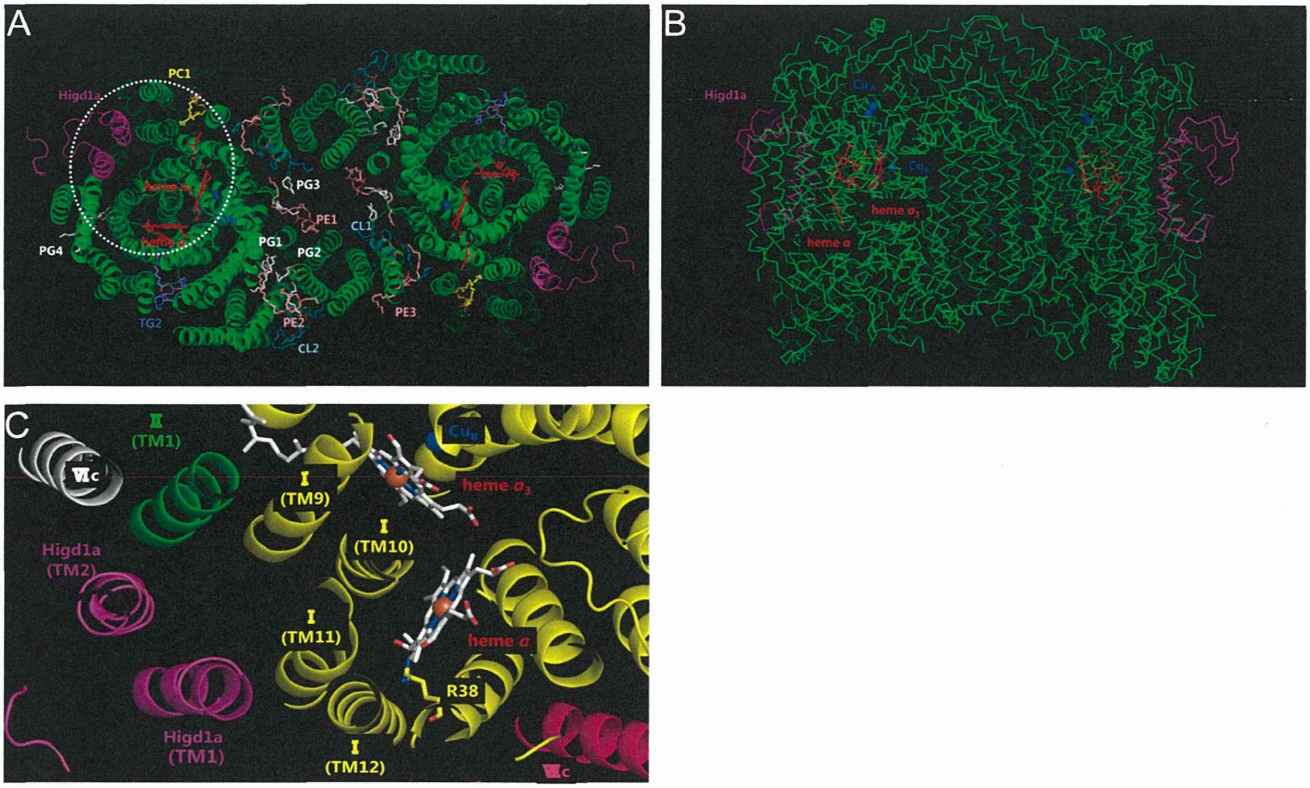

Fig. S10. Docking simulation between CcO (PDB accession code: 3ABM, removal of TG1 and TG3) (the Cα backbone trace: green) and Higd1a (PDB accession code: 2LOM, model 6 of 20 structures) (magenta). Higd1a integrated into the cleft of CcO, just outside of the active center. (*A*) Top view. (*B*) Side view. CL 1–2, cardiolipin (light blue); PC, phosphatidylcholine (yellow); PE 1–3, phosphatidylethanolamine (pink); PG 1–4, phosphatidylglycerol (white); and TG 2, triglyceride. (*C*) Enlarged image of docking simulation (dotted white circle in *A*). The TM1 of Higd1a (magenta) is near the TM11 and TM12 of subunit I (yellow) and it is likely that the binding of Higd1a affects the structure of R38 (yellow) and formyl group of heme *a*.

Hypertension Research (2014) 37, 716–723

www.nature.com/hr

ORIGINAL ARTICLE

Carperitide induces coronary vasodilation and limits infarct size in canine ischemic hearts: role of NO

Hiroshi Asanuma[1,2], Shoji Sanada[3], Masanori Asakura[2], Yoshihiro Asano[3,4], Jiyoong Kim[2], Yoshiro Shinozaki[5], Hidezo Mori[5], Tetsuo Minamino[3], Seiji Takashima[3,4] and Masafumi Kitakaze[2]

Carperitide is effective for heart failure (HF) owing to its diuretic and vasodilatory effects. This recombinant peptide may also have direct cardioprotective effects because carperitide reduces the severity of heart failure and limits infarct size. Because coronary vasodilation is an important cardioprotective treatment modality, we investigated whether carperitide increased coronary blood flow (CBF) and improved myocardial metabolic and contractile dysfunction during ischemia in canine hearts. We also tested whether carperitide is directly responsible for limiting the infarct size. We infused carperitide at 0.025–0.2 μg kg^{-1} min^{-1} into the canine coronary artery. A minimum dose of 0.1 μg kg^{-1} min^{-1} was required to obtain maximal vasodilation. To test the effects of carperitide on ischemic hearts, we reduced perfusion pressure in the left anterior descending coronary artery such that CBF decreased to one-third of the baseline value. At 10 min after carperitide was infused at a dose of 0.1 μg kg^{-1} min^{-1}, we observed increases in CBF, fractional shortening (FS) and pH levels in coronary venous blood without concomitant increases in cardiac nitric oxide (NO) levels; these changes were attenuated using either the atrial natriuretic peptide receptor antagonist HS-142-1 or the NO synthase inhibitor L$^{\omega}$-nitroarginine methyl ester (L-NAME). Cyclic guanosine monophosphate (GMP) levels in the coronary artery were elevated in response to carperitide that also limited the infarct size after 90 min of ischemia and subsequent reperfusion. Again, these effects were blunted by L-NAME. Carperitide increases CBF, reduces myocardial contractile and metabolic dysfunction and limits infarct size. In addition, NO is necessary for carperitide-induced vasodilation and cardioprotection in ischemic hearts.
Hypertension Research (2014) **37**, 716–723; doi:10.1038/hr.2014.70; published online 3 April 2014

Keywords: atrial natriuretic peptide; coronary blood flow; cyclic GMP levels; ischemic hearts; nitric oxide

INTRODUCTION

Despite effective medical therapies, heart failure (HF) remains a major cause of morbidity and mortality worldwide.[1–3] Importantly, ischemic heart disease is a major cause of HF.[4] Significant clinical efforts, therefore, are directed at preventing acute myocardial infarction (AMI) via coronary vasodilation and, in individuals experiencing AMI, reducing the size of the infarct and ischemia/reperfusion injury.[5] The endogenous protein hormone atrial natriuretic peptide (ANP) is mainly released from atrial tissue, and carperitide—recombinant human ANP—is widely used in patients with HF.[6–8] The beneficial effects of carperitide have been attributed to various cardiovascular-protective activities, including diuresis, natriuresis, vasodilatation and reduced activity in the sympathetic nervous system and renin–angiotensin–aldosterone system.[9] Recently, we showed that carperitide limits infarct size and improves cardiac function in patients with AMI (J-WIND study).[10] Among the many cardioprotective effects of carperitide, the most prominent in ischemic heart disease is coronary vasodilation. Because carperitide shares a signaling pathway with nitric oxide (NO),[9,11] and the two molecules are known to interact,[12–14] we hypothesized that carperitide increases coronary blood flow (CBF) in ischemic hearts and that inhibiting endogenous NO signaling would blunt the observed coronary vasodilation.

To test these hypotheses, we determined whether carperitide mediates vasodilation and attenuates the severity of metabolic and contractile dysfunction in ischemic canine hearts. We also examined the role of endogenous NO in these effects. Finally, we investigated carperitide-mediated limitations of the infarct size and whether NO contributes to this cardioprotective activity.

METHODS

Instrumentation

Female beagle dogs weighing 10–14 kg were anesthetized with intravenous pentobarbital sodium (30 mg kg^{-1}). Preparative methods are detailed in a previous study.[15] After the chest was opened, coronary perfusion pressure (CPP) and CBF to the perfused myocardium were measured. A pair

[1]Department of Cardiovascular Science and Technology, Kyoto Prefectural University School of Medicine, Kyoto, Japan; [2]Department of Cardiovascular Medicine, National Cerebral and Cardiovascular Center, Suita, Japan; [3]Department of Cardiovascular Medicine, Osaka University Graduate School of Medicine, Suita, Japan; [4]Department of Medical Biochemistry, Osaka University Graduate School of Medicine, Suita, Japan and [5]Department of Physiology, Tokai University Graduate School of Medicine, Isehara, Japan
Correspondence: Dr M Kitakaze, Department of Cardiovascular Medicine, National Cerebral and Cardiovascular Center, 5-7-1, Fujishirodai, Suita, Osaka, 565-8565, Japan.
E-mail: kitakaze@zf6.so-net.ne.jp
Received 10 December 2013; revised 5 February 2014; accepted 7 February 2014; published online 3 April 2014

of ultrasonic crystals was inserted ~1 cm apart in the inner one-third of the myocardium to measure the myocardial segment length with an ultrasonic dimension gauge.

All procedures complied with the Guide for the Care and Use of Laboratory Animals (NIH publication no. 85–23, 1996 revision) and were approved by the National Cerebral and Cardiovascular Center Committee for Laboratory Animal Use.

Experimental protocols

Protocol I: effects of carperitide on coronary vasodilation in nonischemic hearts. Five dogs were used in this protocol. Coronary arterial and venous blood was sampled for blood gas analysis. Myocardial oxygen consumption (ml per 100 g per min) is calculated by CBF (ml per 100 g per min) × the oxygen difference between coronary arterial and venous blood (ml dl^{-1}). We measured CPP and CBF after dogs were randomly administered carperitide at a dose of 0.025, 0.05, 0.1 or 0.2 $\mu g\,kg^{-1}\,min^{-1}$ (Daiichi-Sankyo KK, Tokyo, Japan) into the left anterior descending coronary artery (LAD). A preliminary study showed that CBF stabilized 5–10 min after a change in the carperitide dose.

Protocol II: effects of carperitide on myocardial ischemia produced by coronary hypoperfusion with or without an ANP receptor antagonist. Twelve dogs were used in this protocol. Coronary arterial and venous blood was sampled for analysis of blood gas and the levels of lactate and plasma NO metabolites (nitrate and nitrite). The following hemodynamic parameters were measured: left ventricular pressure, dP/dt and the segmental length of the perfused myocardium. After hemodynamic parameters were stabilized, we infused either saline ($n=7$) or the ANP receptor antagonist HS-142-1 (40 $\mu g\,kg^{-1}\,min^{-1}$, $n=5$). At 5 min after infusion onset, an occluder attached to the extracorporeal bypass tube was used to reduce CPP such that CBF decreased to one-third of the control value. Thereafter, the occluder was adjusted to maintain CPP at this level. We confirmed that 10 min was required to obtain a stable state in the hypoperfused myocardium. After 10 min, carperitide (0.1 $\mu g\,kg^{-1}\,min^{-1}$) was infused into the LAD and all hemodynamic and metabolic parameters were measured again after 20 min. After acquiring the data, carperitide infusion was discontinued and all hemodynamic and metabolic parameters were measured after 20 min.

We injected microspheres before (10 min after the onset of coronary hypoperfusion), during (30 min) and after (50 min) carperitide infusion.

Protocol III: effects of carperitide on myocardial ischemia produced by coronary hypoperfusion with or without a NO synthase inhibitor. Twelve dogs were used in this protocol. We measured the same hemodynamic and metabolic parameters described in protocol II. We infused either saline ($n=7$) or L^{ω}-nitroarginine methyl ester (L-NAME), an inhibitor of NO synthase (NOS; 10 $\mu g\,kg^{-1}\,min^{-1}$; $n=5$). At 5 min after infusion onset, CPP was reduced such that CBF decreased to one-third of the control value. Thereafter, the occluder was adjusted to maintain CPP at this level. After 10 min, carperitide (0.1 $\mu g\,kg^{-1}\,min^{-1}$) was infused into the LAD and all hemodynamic and metabolic parameters were measured again after 20 min. After acquiring the data, carperitide infusion was discontinued and all hemodynamic and metabolic parameters were measured after 20 min.

Protocol IV: effects of carperitide on cyclic GMP levels in epicardial coronary arteries of ischemic hearts. We determined whether carperitide increases coronary arterial cyclic guanosine monophosphate (GMP) levels in ischemic myocardium. An occluder attached at the extracorporeal bypass tube was used to reduce CPP such that CBF decreased to one-third of control CBF. Thereafter, the occluder was adjusted to maintain CPP at the low level. After 10 min, carperitide (0.1 $\mu g\,kg^{-1}\,min^{-1}$) was infused into the LAD for 10 min and the epicardial LAD (ischemic region) and left circumflex (nonischemic control region) coronary arteries were rapidly removed in the presence ($n=5$) or absence ($n=7$) of L-NAME using precooled stainless steel scissors and tongs. Samples were quickly stored in liquid nitrogen.

Protocol V: effects of carperitide on myocardial infarct size following coronary occlusion and reperfusion. In 36 dogs, the bypass tube to the LAD was occluded for 90 min, followed by reperfusion for 6 h as saline, carperitide (0.1 $\mu g\,kg^{-1}\,min^{-1}$), L-NAME (10 $\mu g\,kg^{-1}\,min^{-1}$) with carperitide (0.1 $\mu g\,kg^{-1}\,min^{-1}$) and L-NAME (10 $\mu g\,kg^{-1}\,min^{-1}$) were administered ($n=9$ for each group) from 10 min before occlusion until 1 h after reperfusion onset, except at the time of coronary occlusion. In all groups, infarct size was assessed 6 h after reperfusion onset.

The area affected by myocardial necrosis and the area at risk were measured in the dogs after protocol completion by an individual who had no knowledge of the specific treatment given to each animal. Infarct size is expressed as a percentage of the area at risk. Regional myocardial blood flow was determined as described previously.[16] Microspheres were administered 80 min after the onset of coronary occlusion.

Assays

Lactate was assessed using an enzymatic assay, and the lactate extraction ratio was obtained as the coronary arteriovenous difference in the lactate concentration multiplied by 100 and divided by the arterial lactate concentration. Levels of plasma NO metabolites (nitrate and nitrite) were analyzed using an automated procedure based on the Griess reaction.[17] Nitrate and nitrite concentration differences between coronary venous and arterial blood were used to quantify cardiac NO levels.

The method used to measure cyclic GMP levels has been described previously.[18] After removing adventitial connective tissues from the coronary arteries (20–40 mg), frozen tissue was powdered, homogenized at 4 °C in 1 ml of ice-cold 6% trichloroacetic acid and centrifuged at 2500 × *g* for 20 min. The supernatant was removed, extracted three times with 3 ml of diethyl ether saturated with water and stored at −80 °C. Cyclic GMP concentrations in the supernatant were measured within 7 days using a radioimmunoassay. Briefly, 100 µl of dioxane–triethylamine mixture containing succinic acid anhydride was used to succinylate cyclic GMP in 100 µl of supernatant. After a 10-min incubation, the reaction mixture was combined with 800 µl of 0.3 M imidazole buffer (pH 6.5). Then, 100 µl of succinyl cyclic GMP tyrosine methyl ester iodinated with ^{125}I (15 000–20 000 counts per min) was added to the assay mixture containing 100 µl of the supernatant and 100 µl of diluted anti-sera in the presence of chloramines. The mixture was kept at 4 °C for 24 h. A cold solution of dextran-coated charcoal (500 µl) was added to the mixture in an ice-cold water bath. The charcoal was spun down, and 0.5 ml of the supernatant was assessed for radioactivity in a gamma spectrometer. Cyclic GMP levels were normalized based on protein content in the coronary artery that was assayed using the Lowry method.[19]

Measurements of regional CBF

Regional myocardial blood flow was determined using a microsphere-based technique as previously reported.[20] Nonradioactive microspheres (Sekisui Plastic, Tokyo, Japan) are made of inert plastic labeled with different stable heavy elements as described in detail in previous studies.[16,20] Microspheres were suspended in isotonic saline with 0.01% Tween-80 to prevent aggregation. Microspheres were ultrasonicated for 5 min followed by 5 min of vortexing immediately before injection. Approximately 1 ml of the microsphere suspension ($2–4 \times 10^5$ spheres per ml) was injected into the left atrium followed by several warm (37 °C) saline flushes (5 ml).

X-ray fluorescence of stable heavy elements was measured using a wavelength dispersive spectrometer (PW 1480; Phillips Co. Ltd., Almelo, Netherlands). This X-ray fluorescence spectrometer has been previously described in detail. In brief, when microspheres are irradiated by the primary X-ray beam, electrons fall back to a lower orbit and emit measurable energy as characteristic fluorescence depending on the element. Therefore, X-ray fluorescence from several differently labeled microspheres in the mixture can be assessed. In protocol II, myocardial blood flow in the endocardium versus that in the epicardium (End/Epi flow ratio) was calculated and normalized based on the wet weight of the sampled myocardium. In protocol V, regional myocardial blood flow was calculated according to the following formula: time flow = tissue count × reference flow/reference count. The results are expressed in ml min^{-1} per g of wet sample.

Statistical analysis

Statistical analysis was performed using two-way analysis of variance[21,22] to compare data among the groups. When analysis of variance reached significance, paired data were compared using Bonferroni's test. Changes in the hemodynamic and metabolic parameters over time were compared by analysis of variance for repeated measures. Analysis of covariance, by endocardial collateral blood flow in the inner half of left ventricle wall as the covariate, was used to account for the effect of endocardial collateral blood flow on infarct size. All results are expressed as mean ± s.e.m., and $P<0.05$ was considered significant.

RESULTS

Mean blood pressure (103 ± 2 mm Hg) and heart rate (139 ± 2 beats per min) did not differ significantly among the groups. These systemic hemodynamic parameters did not change significantly before, during or after coronary hypoperfusion or complete coronary occlusion with or without administration of a pharmacologic agent.

Effects of carperitide on CBF in nonischemic hearts

Figure 1 shows CBF during infusions of carperitide. CBF increased based on the dose of carperitide, with saturation of coronary vasodilation observed at a dose of 0.1 $\mu g\,kg^{-1}\,min^{-1}$ (Figure 1a) despite no changes in CPP (102 ± 2 mm Hg) or myocardial oxygen consumption (Figure 1b).

Effects of carperitide on CBF and the severity of myocardial ischemia

Figure 2 shows CBF (Figure 2b) and fractional shortening (FS) (Figure 2c) whereas CPP was reduced (Figure 2a) with or without the denoted pharmacologic agents. Carperitide increased both CBF and FS whereas CPP was held constant, effects that were blunted by the ANP receptor antagonist HS-142-1. The myocardial End/Epi flow ratio was also augmented by carperitide (Figure 3). Carperitide increased both lactate extraction ratio (Figure 4a) and pH levels (Figure 4b) in coronary venous blood from the ischemic area; HS-142-1 inhibited these effects without increasing cardiac NOx levels (differences in nitrate and nitrite levels between coronary venous and arterial blood; Figure 4c).

Figure 5 shows CBF (Figure 5b) and FS (Figure 5c) whereas CPP was reduced (Figure 5a) with or without L-NAME. Carperitide increased both CBF and FS without changes in CPP, the effects that were inhibited by an inhibitor of NOS (L-NAME). Carperitide increased both lactate extraction ratio (Figure 6a) and pH levels (Figure 6b) in coronary venous blood from the ischemic area; L-NAME blunted these effects without increasing cardiac NOx levels (Figure 6c).

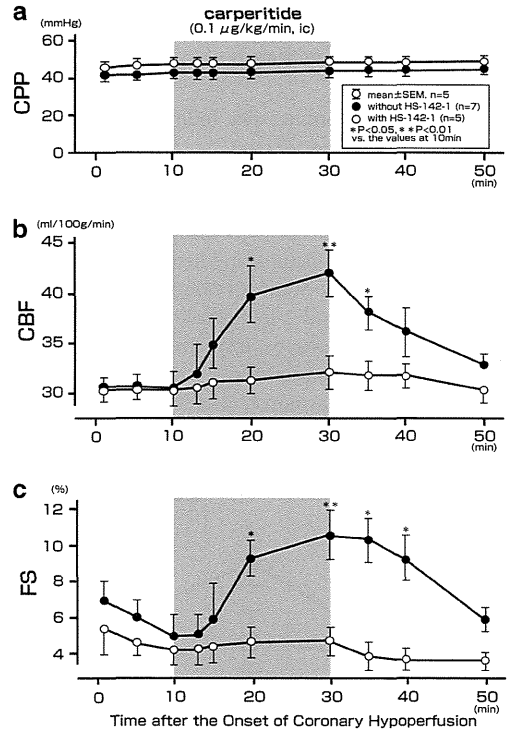

Figure 2 Effects of carperitide on coronary blood flow (CBF) and fractional shortening (FS) in ischemic hearts with or without HS-142-1. Carperitide increased both CBF (**b**) and FS (**c**) whereas coronary perfusion pressure (CPP; **a**) was held constant, effects that were blunted by the atrial natriuretic peptide (ANP) receptor antagonist HS-142-1. $*P<0.05$, $**P<0.01$ *vs.* the values at 10 minutes.

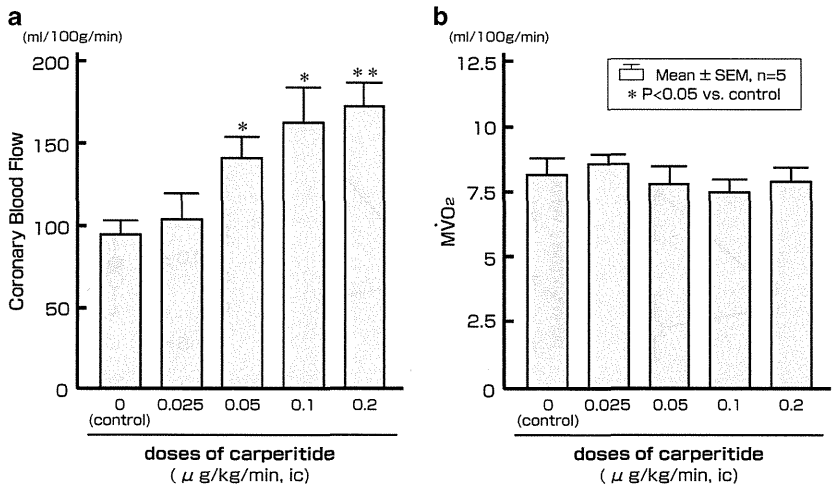

Figure 1 Effects of carperitide on coronary blood flow (CBF) and myocardial oxygen consumption (MVO_2) in nonischemic hearts. CBF increased as the carperitide dose increased (**a**) despite no changes in myocardial oxygen consumption (**b**). $*P<0.05$, $**P<0.01$ *vs.* the control.

We also investigated cyclic GMP levels during carperitide-induced coronary vasodilation. Without carperitide treatment, myocardial ischemia (CPP: 105 ± 4 to 42 ± 2 mm Hg; CBF: 82 ± 3 to 27 ± 2 ml per 100 g per min) increased cyclic GMP concentrations in the coronary artery from 44 ± 17 to 121 ± 22 fmol per mg protein (Figure 7; $P<0.01$). Moreover, carperitide provided during myocardial ischemia further increased cyclic GMP levels in the involved coronary artery ($P<0.05$); L-NAME attenuated this effect. Furthermore, carperitide increased myocardial cyclic GMP levels (168 ± 30 to 263 ± 30 pmol per mg protein, $n=3$ each); L-NAME attenuated this effect (184 ± 24 pmol per mg protein, $n=3$).

Effects of carperitide on infarct size following ischemia and reperfusion

Of the 36 dogs, 6 were excluded from the analysis because their subendocardial collateral flow was >15 ml per 100 g per min, and hence 30 dogs completed the protocol satisfactorily. Of these 30 dogs, 6 developed ventricular fibrillation, and hence these animals were also excluded from analysis. The number of dogs that were excluded from the analysis were 2, 0, 2 and 2 in the saline, carperitide, carperitide and L-NAME or L-NAME groups, respectively.

Heart rate and aortic blood pressure were similar among the four groups throughout this protocol. Neither the area at risk nor endocardial collateral blood flow in the LAD region during myocardial ischemia differed among the groups receiving saline, carperitide, carperitide and L-NAME or L-NAME (Table 1). Carperitide, however, decreased the infarct size compared with results from the group treated with saline (18.1 ± 3.6% vs. 39.8 ± 5.1% of the area at risk, respectively; $P<0.05$); this effect was blunted by L-NAME (18.1 ± 3.6% vs. 41.6 ± 2.2% of the area at risk in the groups treated

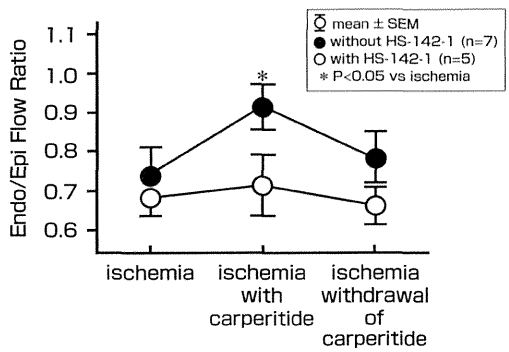

Figure 3 The ratio of epicardial flow to endocardial flow in the myocardium during ischemia. Carperitide predominantly increased endocardial blood flow relative to epicardial blood flow. This effect was attenuated by HS-142-1. *$P<0.05$ *vs. ischemia*.

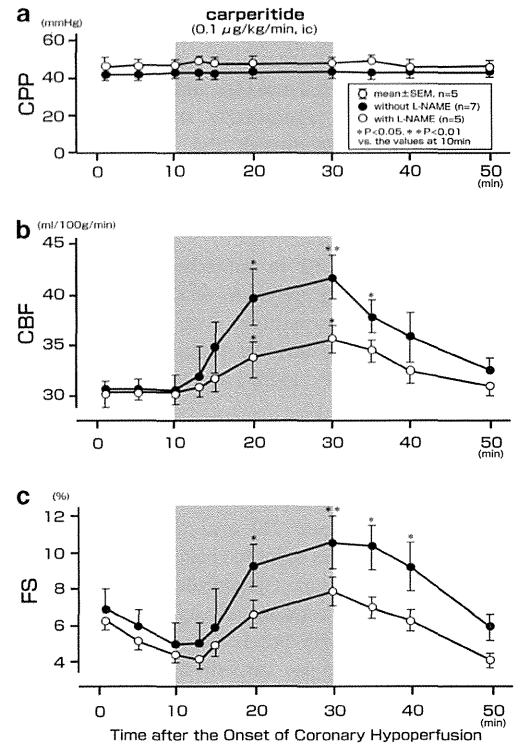

Figure 5 Effects of carperitide on coronary blood flow (CBF) and fractional shortening (FS) in ischemic hearts with or without $L^{(n)}$-nitroarginine methyl ester (L-NAME). Carperitide increased both CBF (**b**) and FS (**c**) without changes in coronary perfusion pressure (CPP; **a**), effects that were inhibited by an inhibitor of nitric oxide (NO) synthase L-NAME. *$P<0.05$, **$P<0.01$ *vs. the values at 10 minutes*.

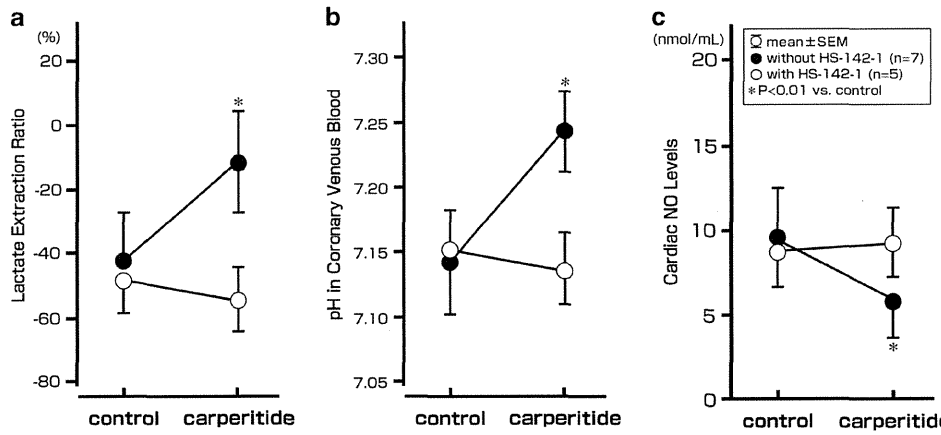

Figure 4 Effects of carperitide on metabolic function in ischemic hearts with or without HS-142-1. Carperitide increased both (**a**) lactate extraction ratio (LER) and (**b**) pH levels in coronary venous blood from the ischemic area; HS-142-1 inhibited these effects without increasing cardiac nitric oxide (NO) levels (**c**). *$P<0.01$ *vs.* the control.